Dalton Transactions

Accepted Manuscript

ROYAL SOCIETY OF CHEMISTRY

www.rsc.org/dalton

Journal Name

ARTICLE

A zwitterionic 1D/2D polymer co-crystal and its polymorphic sub-components: a highly selective sensing platform for HIV ds-DNA sequences

Cite this: Dalton Trans., xxxx, xx, xxxx

Hai-Qing Zhao,‡[a] Shui-Ping Yang,‡[a] Ni-Ni Ding,[bc] Liang Qin,[a] Gui-Hua Qiu,[a] Jin-Xiang Chen,*[a] Wen-Hua Zhang,*[bc] Wen-Hua Chen*[a] and T. S. Andy Hor*[cd]

Received 00th January 20xx,

Accepted 00th January 20xx

DOI: 10.1039/x0xx00000x

www.rsc.org/

Polymorphic compounds $\{[Cu(dcbb)_2(H_2O)_2]\cdot 10H_2O\}_n$ (**2**, 1D chain), $[Cu(dcbb)_2]_n$ (**3**, 2D layer) and their co-crystal $\{[Cu(dcbb)_2(H_2O)][Cu(dcbb)_2]_2\}_n$ (**4**) have been prepared from the coordination reaction of a 2D polymer $[Na(dcbb)(H_2O)]_n$ (**1**, H_2dcbbBr = 1-(3,5-dicarboxybenzyl)-4,4'-bipyridinium bromide) with $Cu(NO_3)_2\cdot 3H_2O$ at different temperatures in water. Compounds **2**–**4** have identical metal-to-ligand stoichiometric ratio of 1:2, but absolutely differ in structure. Compound **3** features a 2D layer structure with aromatic rings, positively charged pyridinium and free carboxylates on its surface, promoting electrostatic, π-stacking and/or hydrogen-bonding interactions with the carboxyfluorescein (FAM) labeled probe single-stranded DNA (probe ss-DNA, delineates as P-DNA). The resultant P-DNA@**3** system facilitated fluorescence quenching of FAM *via* a photoinduced electron transfer process. The P-DNA@**3** system functions as an efficient fluorescent sensor selective for HIV double-stranded DNA (HIV ds-DNA) due to the formation of rigid triplex structure with the recovery of FAM fluorescence. The system reported herein also distinguishes complementary HIV ds-DNA from mismatched target DNA sequences with the detection limit of 1.42 nM.

Introduction

Developing materials for assaying biomolecules has recently received increasing attention due to the merits of high sensitivity, selectivity, operational convenience, as well as their potential applications in clinical diagnosis and therapeutic advances.[1] To date, numerous materials have been adopted as sensors for biomolecules, including macroporous silica, carbon nanomaterials (CNMs) and porous organic frameworks.[2] Metal–organic frameworks (MOFs) have also been recently used as sensing platforms for biomolecules.[3] In 2013, Chen *et al.* reported the first example of a 2D MOF, $Cu(H_2dtoa)$ (H_2dtoa = *N*,*N*'-bis(2- hydroxyethyl)dithiooxamide) for the detection of proteins and nucleic acids.[4] To date, a limited number of MOFs, such as MIL-101,[3e] UiO-66,[3h] and UiO-66-NH_2[3f, 3g] have been evaluated for DNA/RNA detection. A common challenge is the inherent poor stability of most reported MOFs, which have restricted their activities in biological media, for example, biomedia of tris-HCl buffer solution in the presence of NaCl and $MgCl_2$.[5]

In recent years, we have been keenly interested in coordination compounds based on quaternized-carboxylate ligands (Chart 1). We have shown that a diverse framework materials assembled from these ligands exhibited high moisture and water stability, as well as potent DNA binding activity and sensing for ebolavirus RNA sequences.[6] We herein report the evaluation of a unique polymorphic system containing three MOFs, namely $\{[Cu(dcbb)_2(H_2O)_2]\cdot 10H_2O\}_n$ (**2**, 1D chain), $[Cu(dcbb)_2]_n$ (**3**, 2D layer) and their co-crystal $\{[Cu(dcbb)_2(H_2O)][Cu(dcbb)_2]_2\}_n$ (**4**). Compounds **2**–**4** are prepared from the coordination reactions of a 2D polymer precursor $[Na(dcbb)(H_2O)]_n$ (**1**, H_2dcbbBr = 1-(3,5-dicarboxybenzyl)-4,4'-bipyridinium bromide, Chart 1) with $Cu(NO_3)_2$ at different temperatures in water. They have the same ligand-to-metal stoichiometric ratio but differ in structure. Their compositional similarity enables us to focus on the net structural contributions to their biological performances. Of the three Cu(II) materials, **3** effectively binds probe DNA (P-DNA) and further distinguishes its complementary counterparts HIV ds-DNA over mismatched target DNA with the detection limit of 1.42 nM.

[a] *Guangdong Provincial Key Laboratory of New Drug Screening, School of Pharmaceutical Sciences, Southern Medical University, Guangzhou 510515, P. R. China. Fax: +86-20-61648533; E-mail: jxchen@smu.edu.cn, whchen@smu.edu.cn*

[b] *College of Chemistry, Chemical Engineering and Materials Science, Soochow University, Suzhou 215123, China. Email: whzhang@suda.edu.cn*

[c] *Institute of Materials Research and Engineering (IMRE), A*STAR, 3 Research Link, 117602, Singapore*

[d] *Department of Chemistry, National University of Singapore, 3 Science Drive 3, 117543, Singapore; E-mail: andyhor@hku.hk*

†Electronic Supplementary Information (ESI) available: PXRD patterns of compounds **1**–**4**, 2D network extended in the *ab* plane of **1**, fluorescence quenching of the probe DNA by $Cu(NO_3)_2$, fluorescent recovery of P-DNA@$Cu(NO_3)_2$ system by target HIV ds-DNA and influence of incubation time between the P-DNA@**3** system and the target ds-DNA on fluorescence intensity. CCDC numbers 1420147-1420150 for **1**–**4**. These materials are available free of charge via the internet at http://pubs.acs.org. For ESI and crystallographic data in CIF format, see DOI:10.1039/c000000x/

‡ These authors contributed equally to this work.

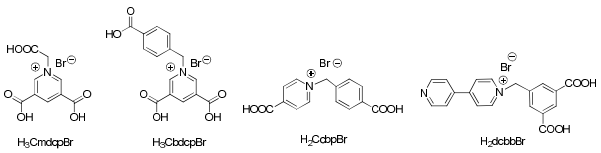

Chart 1. Structures of quaternized-carboxylate ligands H_3CmdcpBr, H_3CbdcpBr, H_2CcbBr, and H_2dcbbBr.

Experimental

General procedures

^{1}H spectra (CD_3OD solvents) were recorded on Varian Mercury 400 spectrometer. IR spectra were recorded on a Nicolet MagNa-IR 550 infrared spectrometer. Elemental analyses for C, H and N were performed on an EA1112 CHNS elemental analyzer. Thermogravimetric analyses (TGA) were performed on a TA instruments Q500 thermogravimetric analyzer at a heating rate of 10 °C/min under a nitrogen gas flow in an Al_2O_3 pan. The fluorescence spectra and fluorescence anisotropy was measured on LS55 fluorescence spectrophotometer. Zeta potential measurement was carried out on Nano ZS90 zetasizer. Powder X-ray diffraction (PXRD) was recorded on a Rigaku D/max-2200/PC. The X-ray generated from a sealed Cu tube was mono-chromated by a graphite crystal and collimated by a 0.5 mm MONOCAP (λ Cu-Kα = 1.54178 Å). The tube voltage and current were 40 kV and 40 mA, respectively. Samples for PXRD were prepared by placing thin layers of samples on zero-background silicon (510) crystal plates.

All the reagents and solvents were obtained from commercial sources and used without further purification. The DNA sequences were purchased from Sangon Inc. (Shanghai, China) and are shown as follows:

Probe DNA: 5'-FAM-TTCTTCTTTTTTCT-3'
Complementary target HIV ds-DNA T_0 (ds-DNA-1,2):
5'-CGAGTTAAGAAGAAAAAAGATTGAGC-3'/5'-GCTCAATCTTTTTTCTTCTTAACTCG-3'
One base pair mutated T_1 (ds-DNA-3,4):
5'-CGAGTTAAGAAAAAAAAAGATTGAGC-3'/5'-GCTCAATCTTTTTTTTTCTTAACTCG-3'
Complementary ss-DNA T_2: 5'-AGAAAAAAGAAGAA-3'
One base pair mutated for complementary ss-DNA T_3:
5'-AGAACAAAGAAGAA-3'
Non-specific ss-DNA T_4:
5'-GCTAGAGATTTTCCACACTGACT-3'
Duplex DNAs were prepared according to the previous reports.[5a, 7] All the DNA samples were dissolved in 100 nM Tris-HCl buffer solution (pH 7.4, 100 mM NaCl, 5 mM $MgCl_2$) and stored at 4 °C for use.

Synthesis of ligand H_2dcbbBr and compounds 1–4

Synthesis of H_2dcbbBr

A solution of 5-(bromomethyl)-isophthatic acid (5.18 g, 20 mmol) in DMF (25 mL) was added dropwise to a solution of 4,4'-bipyridine (3.74 g, 24 mmol) in DMF (10 mL). The resulting mixture was stirred at 70 ºC for 12 h and the white precipitates formed were collected by filtration and washed with DMF (30 mL) and acetone (15 mL) to afford H_2dcbbBr (7.64 g, 92%). Anal. Calcd. for $C_{19}H_{15}N_2O_4Br$: C 54.96, H 3.64, N 6.75. Found: C 54.68, H 3.57, N 6.92. IR (KBr disc, cm^{-1}) *v* 3424 (s), 3063 (s), 2503 (m), 1955 (m), 1702 (s), 1645 (s), 1604 (s), 1548 (m), 1412 (s), 1331 (m), 1278 (s), 1261 (s), 1166 (m), 1071 (s), 1002 (s), 817 (s), 751 (s), 631 (s).

Synthesis of $[Na(dcbb)(H_2O)]_n$ (1)

H_2dcbbBr (4 mmol, 1.66 g) was suspended in MeOH (50 mL) and the pH adjusted to 7.0 with 0.1 M NaOH solution to give a clear green solution. For the H_2O is very small component with MeOH and can be ignored, diethyl ether (100 mL) was allowed to diffuse into the MeOH/H_2O solution to provide light green crystals of **1**, which were collected by filtration and dried *in vacuo*. Yield: 2.87 g (75%). ^{1}H-NMR (400 MHz, CD_3OD) δ 9.23 (d, *J* = 7.2 Hz, 2H), 8.83 (dd, *J* = 1.6 and 1.6 Hz, 2H), 8.64 (s, 1H), 8.54 (d, *J* = 6.8 Hz, 2H), 8.06 (d, *J* = 0.8 Hz, 2H), 8.00 (dd, *J* = 1.6 and 1.6 Hz, 2H), 5.98 (s, 2H). Anal. Calcd. for $C_{19}H_{15}NaN_2O_5$: C 60.96, H 4.04, N 7.48. Found: C 60.58, H 3.98, N 7.37. IR (KBr disc, cm^{-1}) *v* 3410 (s), 1662 (s), 1625 (s), 1608 (s), 1546 (s), 1390 (s), 1357 (s), 1226 (m), 1167 (w), 1103 (w), 1020 (w), 912 (w), 852 (w), 817 (w), 770 (m), 726 (m), 707 (s), 642 (m), 507 (m), 462 (m).

Synthesis of compounds 2−4

A solution of compound **1** (74.8 mg, 0.2 mmol) in H_2O (70 mL) was added to $Cu(NO_3)_2{\cdot}3H_2O$ (24.0 mg, 0.1 mmol) in H_2O (40 mL). The resulting mixture was stirred for 0.5 h at room temperature to provide a clear light green solution 1.

$\{[Cu(dcbb)_2]{\cdot}10H_2O\}_n$ (2). The abovementioned solution 1 was placed in DURAN laboratory bottle and sealed with blue PP screw cap and pouring ring. The bottle was transferred into a programmable oven. The sample temperature of the oven was increased smoothly from 25 ºC to 100 ºC in 4 h, kept at 100 ºC for 72 h and then cooled to room temperature within 48 h. The blue needle crystals was formed and washed with MeOH to give compound **2** (161 mg, 85%). Anal. Calcd. for $C_{38}H_{50}CuN_4O_{20}{\cdot}4.5H_2O$: C 44.42, H 5.79, N 5.45. Found: C 44.58, H 5.60, N 5.06. IR (KBr disc, cm^{-1}) *v* 3412 (s), 3053 (s), 1617 (s), 1570 (s), 1495 (w), 1416 (m), 1385 (s), 1362 (s), 1221 (w), 1158 (w), 1075 (w), 822 (m), 780 (m), 723 (m), 644 (w).

$[Cu(dcbb)_2]_n$ (3). The abovementioned solution 1 was placed in DURAN laboratory bottle and sealed with blue PP screw cap and pouring ring. The bottle was transferred into a programmable oven. The sample temperature of the oven was increased smoothly from 25 ºC to 85 ºC in 4 h, kept at 85 ºC for 72 h and then cooled to room temperature within 48 h. The blue needle crystals was formed and washed with MeOH to give compound **3** (120 mg, 82%). Anal. Calcd. for $C_{38}H_{26}CuN_4O_8{\cdot}15H_2O$: C 45.62, H 5.64, N 5.60. Found: C 45.22, H 5.67, N 5.88. IR (KBr disc, cm^{-1}) *v* 3399 (s), 3056 (s), 1641 (s), 1615 (s), 1567 (s), 1454 (w), 1407 (m), 1363 (s), 1224 (w), 1164 (m), 1079 (w), 823 (s), 783 (m), 721 (s), 640 (w).

$\{[Cu(dcbb)_2(H_2O)][Cu(dcbb)_2]_2\}_n$ (4). The abovementioned solution 1 was allowed to stand for two weeks at room temperature to give green block crystals. The crystals were collected and washed with MeOH to give compound **4** (189 mg, 92%). Anal. Calcd. for $C_{114}H_{78}Cu_3N_{12}O_{25}{\cdot}14.5H_2O$: C 55.48, H 4.37, N 6.81. Found: C 55.09, H 3.90, N 6.51. IR (KBr disc, cm^{-1}) *v* 3402 (s), 3116 (s), 1636 (s), 1618 (s), 1570 (s), 1458 (m), 1412 (s), 1362 (s), 1220 (m), 1161 (m), 1076 (w), 821 (s), 781 (s), 720 (s), 640 (w).

X-ray crystal structure determinations

Crystallographic measurements were made on a Bruker APEX II diffractometer by using graphite-monochromated Mo Kα (λ = 0.71073 Å) irradiation for **1**–**4**. The data were corrected for Lorentz and polarization effects with the SMART program and for absorption effects with SADABS.[8] All crystal structures were solved by direct methods and refined on F^2 by full-matrix least-squares techniques with SHELXTL–97 program.[9] In **1** and **2**, the location of the hydrogen atoms on the coordinated water were suggested by Calc-OH program in WinGX suite,[10] their O–H distances were further restrained to O–H = 0.85 Å and thermal parameters constrained to $U_{iso}(H) = 1.2U_{eq}(O)$. In **2**, one of the free water (O6W) lies on a special position of higher symmetry than the

molecule can possess. They are treated as spatial disorder but applying PART –1 and PART 0 in the *.ins* file with the site occupation factors changed to 0.50 for the molecule. The occupancy factor for O7W was fixed at 0.5 to obtain reasonable thermal factors. In **3**, one of the carboxylates (C27, O7 and O8) adopts positional disorder with the relative ratio of 0.78/0.22 refined for the two components. A large amount of electron density in the lattice was found for ordered and disordered water molecules. The solvent contribution was then modeled using SQUEEZE in the Platon program suite.[11] In **4**, the whole Cu2 based moiety adopts a symmetry disorder and the symmetry suppressed by applying PART –1 instruction in the *.ins* file followed by changing the occupancy factor for each atom to 0.50. Significant restraints/constraints were applied for the Cu2-based moiety, which include the fixation of all aromatic rings to ideal hexagonal. The thermal parameters of some atoms are averaged using EADP constraint where necessary. A large amount of spatially delocalized electron density in the lattice was found but acceptable refinement results could not be obtained for this electron density. The solvent contribution was then modeled using SQUEEZE in the Platon program suite. A summary of the key crystallographic information for **1**–**4** was summarized tabulated in Table 1. Selected bond distances (Å) and angles (º) for compounds **1**–**4** are listed in Table S1.

HIV DNA detection experiments

The emission spectra were collected from 500 to 650 nm under excitation at 480 nm. The excitation slit width was 3.0 nm and emission slit width 5.0 nm. The fluorescence intensity at 518 nm was used for quantitative analysis.

Firstly, fluorescence quenching experiments of P-DNA by compounds **2**−**4**, H_2dcbbBr and $Cu(NO_3)_2$ were performed by keeping the concentrations of P-DNA constant, while gradually increasing the concentration of each compound. Specifically, to a solution of P-DNA (70 nM) in 100 nM Tris-HCl (pH 7.4, 100 mM NaCl, 5 mM $MgCl_2$) were added aliquots of a solution of each compound containing P-DNA (70 nM) in the same buffer and oscillated to form P-DNA@compound complex. The corresponding fluorescence spectra were measured until saturation was observed. The quenching efficiency (Q_E, %) was calculated according to Eq. (1).[5a]

$$Q_E\% = (1 - F_M/F_0)\times 100\% \quad (1)$$

Wherein F_M and F_0 are fluorescent intensities at 518 nm in the presence and the absence of each compound, respectively.

Secondly, fluorescence recovery experiments were conducted by adding target DNA of varying concentrations to the above saturated P-DNA@compound solution, at room temperature and the oscillation time was 90 min for each concentration until saturation of fluorescence recovery was observed. Fluorescence recovery efficiency was calculated according to Eq. (2).[5a]

$$R_E = F_T/F_M - 1 \quad (2)$$

Wherein F_T and F_M are fluorescence intensities at 518 nm in the presence and the absence of target DNA, respectively.

Table 1. Crystallographic data for compounds **1**–**4**.

Compound	**1**	**2**	**3**	**4**
Molecular formula	$C_{19}H_{15}N_2NaO_5$	$C_{38}H_{50}CuN_4O_{20}$	$C_{38}H_{26}CuN_4O_8$	$C_{114}H_{78}Cu_3N_{12}O_2$
Formula weight	374.32	946.36	730.17	2206.50
Crystal system	orthorhombic	triclinic	monoclinic	triclinic
Space group	$P2_12_12_1$	P–1	$P2_1/c$	P–1
a (Å)	8.1815(16)	9.4670(9)	9.038(3)	9.0094(10)
b (Å)	10.460(2)	11.0827(11)	38.492(14)	13.6583(13)
c (Å)	19.705(4)	12.4243(12)	13.702(5)	29.581(3)
α (°)	90.00	72.103(2)	90.00	82.577(2)
β (°)	90.00	82.451(2)	95.882(8)	86.380(2)
γ (°)	90.00	66.433(2)	90.00	82.999(2)
V (Å^3)	1686.3(6)	1136.96(19)	4742(3)	3578.5(6)
Z	4	1	4	1
T/K	293(2)	296(2)	153(2)	123(2)
D_{calc} (g cm^{-3})	1.474	1.382	1.023	1.024
λ (Mo-Kα) (Å)	0.71073	0.71073	0.71073	0.71073
μ (cm^{-1})	0.129	0.561	0.504	0.502
Total reflections	16015	9994	44317	15720
Unique reflections	3445	5616	11037	15720
No. observations	2989	4424	6179	11319
No. parameters	241	274	488	682
Flack parameters	0.2(4)	N.A.	N.A.	N.A.
R^a	0.0492	0.0585	0.0893	0.0790
wR^b	0.1004	0.1757	0.2193	0.2119
GOF^c	1.089	1.089	0.957	1.128
$\Delta\rho_{max}$ (e Å^{-3})	0.178	1.356	0.825	2.757
$\Delta\rho_{min}$ (e Å^{-3})	−0.179	−0.579	−0.971	−1.306

[a] $R_1 = \Sigma||F_o|-|F_c||/\Sigma|F_o|$. [b] $wR_2 = \{\Sigma[w(F_o^2-F_c^2)^2]/\Sigma[w(F_o^2)^2]\}^{1/2}$. [c] GOF = $\{\Sigma[w(F_o^2-F_c^2)^2]/(n-p)\}^{1/2}$, where n is the number of reflections and p is total number of parameters refined

Results and discussion

Synthesis and characterizations of 1–4

The precursor compound $[Na(dcbb)(H_2O)]_n$ (**1**) was obtained from the diffusion of Et_2O into a mixture of H_2dcbbBr with NaOH in MeOH. Subsequent coordination reaction of **1** with $Cu(NO_3)_2{\cdot}3H_2O$ in water provided a 1D chain compound $\{[Cu(dcbb)_2(H_2O)_2]{\cdot}10H_2O\}_n$ (**2**) at 100 ºC, a 2D layer compound $[Cu(dcbb)_2]_n$ (**3**) at 85 ºC and their co-crystal form $\{[Cu(dcbb)_2(H_2O)][Cu(dcbb)_2]_2\}_n$ (**4**) at room temperature. The coordination reaction is driven by complexation of Cu(II) and carboxylates.[6i, 12]

Powder X-ray diffraction (PXRD, Figure S1) analysis revealed that the experimental diffraction pattern is in agreement with that of the simulated from single-crystal diffraction data for compound **1**. While for **2**−**4**, PXRD pattern of fresh powder immersed in H_2O for 12 h are in agreement with those of the simulated, indicating their bulky phase purity and water stability. The bulk phase purity for **1**−**4** was further confirmed by elemental analysis.

Crystal structure of $[Na(dcbb)(H_2O)]_n$ (1)

In **1**, the Na atom is coordinated by three carboxylate groups from three dcbb ligands, all in monodentate mode and its tetrahedral coordination geometry is completed by further association of one water solvate (Figure 1a). The Na centers are consecutively linked by one μ–COO along the *b* axis and the other monodentate carboxylate along the *a* axis to give an overall 2D (6,3) network within the *ab* plane (Figures 1b and Figure S2).

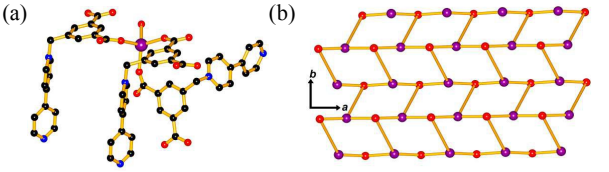

Figure 1. (a) Ball-and-stick model of $[Na(dcbb)(H_2O)]_n$ (**1**) showing the complete coordination sphere of Na. Color codes: Na (violet), O (red), N (blue), C (black). (b) 2D network of **1** extended in the *ab* plane with all the ligands and Na represented by red and violet spheres.

Crystal structure of $\{[Cu(dcbb)_2(H_2O)_2]{\cdot}10H_2O\}_n$ (2)

Compound **2** features a 1D zwitterionic chain with corner-sharing grid propagates along the [−1 0 1] direction and has 1:2 Cu-to-dcbb stoichiometry (Figure 2a). Each Cu center is 6-coordinate, associated by a pair of *trans* located N and a pair of *trans* located O atoms from four dcbb ligands which also define the equatorial plane of an octahedron. Each Cu center is further associated by two aqua molecules at the axial positions to complete its octahedral coordination. Adjacent Cu atoms are bridged by a pair of dcbb ligands in a head-to-tail arrangement. Notably, one of the carboxylates in each ligand is anionic and uncoordinated to neutralize the positive charge generated either by the positive Cu(II) or the pyridinium center, and the chain is thus zwitterionic. The 1D chains of **1** are packed within the cell to generate small channels along the *b* direction (Figure 2b), and these channels are occupied by water molecules.

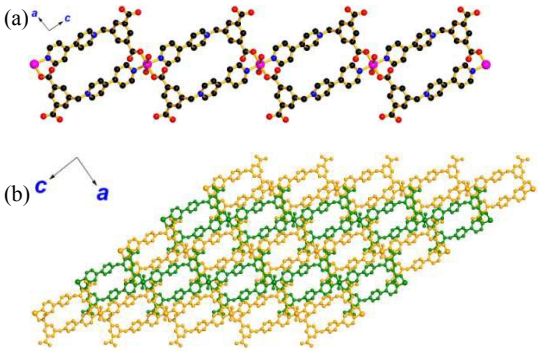

Figure 2. (a) The 1D grid structure of $\{[Cu(dcbb)_2(H_2O)_2]{\cdot}10H_2O\}_n$ (**2**) looking down the *b* axis. (b) The packing diagram of **2** with the color for the adjacent chains set to golden-yellow and green to enhance clarity. All the dissociated water solvates and hydrogen atoms are omitted. Color codes for (a): Cu (dark magenta), O (red), N (blue), C (black).

Crystal structure of $[Cu(dcbb)_2]_n$ (3)

Compound **3** features a 2D layer structure and also has a Cu-to-dcbb ratio of 1:2 in the crystal. As shown in Figure 3a, there are two types of dcbb ligands (delineated as type I and type II). Type I dcbb ligand serves as the tritopic ligand, juxtaposing two Cu centers along *a* direction *via* two carboxylates and an additional Cu center in the *c* direction *via* the pyridyl function. Type II dcbb functions as a ditopic ligand that bridges Cu atoms in *c* direction *via* one carboxylate and one pyridyl groups, leaving the other carboxylate anionic and uncoordinated to neutralize the positive charge. Each Cu is five-coordinate and has a square pyramidal geometry, associated by two *trans* located O atoms from a pair of monodentate carboxylates and two *trans* located N atoms from a pair of pyridyls to define the square of the pyramidal. The apical position of the pyramidal is occupied by one additional O atom from the third monodentate carboxylate. The Cu centers in the *a* direction are connected through dicarboxylate single bridges from type I dcbb ligands. All the pyridyls and one carboxylate from the type II ligand are responsible for chain propagation in the *c* direction. A 2D layer structure is thus formed within the *ac* plane.

One notable feature of **3** is that type I and type II dcbb ligands are located at the two sides of the plane (Figure 3a). Analysis of the cell packing of **3** revealed that these layers exist as pairs in the cell. Type I dcbb ligands pairwise in a face-to-face arrangement (middle two layers in Figure 3b), imposing the type II dcbb ligands to be in face-to-face.

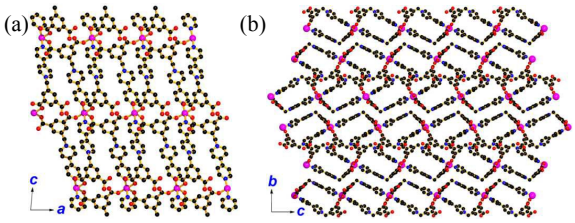

Figure 3. (a) The 2D structure of $[Cu(dcbb)_2]_n$ (**3**) looking down the *b* axis. (b) The packing diagram of **3** looking down *a* axis, showing the double layer pairs and the face-to-face arrangement of the free uncoordinated carboxylates. All disordered domains and hydrogen atoms are omitted. Color codes: Cu (dark magenta), O (red), N (blue), C (black).

Crystal structure of $\{[Cu(dcbb)_2(H_2O)][Cu(dcbb)_2]_2\}_n$ (4)

1D chain of **2** and 2D layer of **3** have the same Cu-to-dcbb stoichiometry also form a co-crystal of **4**. Within **4**, the pairwise nature of the 2D layers are retained and separated by the 1D grids. The overall molecule therefore has a 2D:1D ratio of 2:1 (based on the number of Cu atoms, Figure 4). The 1D grids also display disorder to form a satisfying packing with the 2D layers.

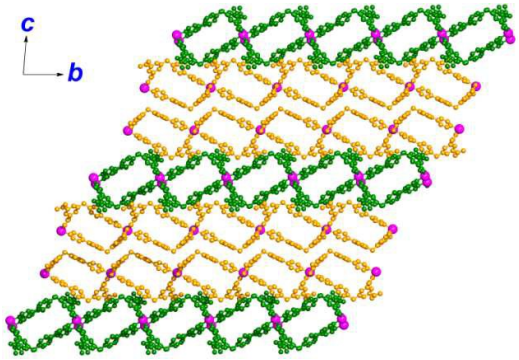

Figure 4. The packing diagram $\{[Cu(dcbb)_2(H_2O)][Cu(dcbb)_2]_2\}_n$ (**4**) looking down *a* axis showing the alternative arrangement of the 1D chains (green) and 2D double layer pairs (golden-yellow). The disordered domains within the 1D chains are maintained and hydrogen atoms omitted.

Polymorphs, co-crystals and salts have been attracting substantial interest in pharmaceutical sciences with inherent connections.[13] Pharmaceutical molecules are often subjected to form salt and/or co-crystals with other ingredients to achieve enhanced solubility, dissolution rate, stability and/or hygroscopicity.[14] However, the integration of polymorphs, co-crystals and salts in one system in MOFs, *viz,* a single salt co-crystal that is composed of two distinctive types of polymorphic sub-components, is rare.[15] The challenge arises from the difficulty in packing two types of polymorphic sub-components in one crystal, particularly when these sub-components are also polymeric. Compound **4** thus represents a rare case that integrates polymorphism (to **2** and **3**), co-crystal (of **2** and **3**) and salt (considering zwitterionic complex as inner salt).

Sensing properties of compounds 2–4 toward HIV ds-DNA

Compounds **1**–**4** are obtained in good yields and are water stable at room temperature. As discussed above, **2**–**4** contain aromatic rings and positively charged pyridinium cation centers. The positively charged skeleton is known to promote electrostatic interactions with the DNA backbone. Such electrostatic interactions is further strengthened by the presence of cationic metal centers.[16] Thus, compounds **2**–**4** may form electrostatic and π-stacking interactions with ss-DNA chains, as the latter is composed of aromatic entities laced up by an anionic phosphate-based chain.[17] Such interaction may quench the fluorescence of the dye-tagged ss-DNA.[4] To test this hypothesis, we chose fluorophore FAM-labeled ss-DNA 5'-FAM-TTCTTCTTTTTTCT-3' as a P-DNA (FAM = carboxyfluorescein), which is the complementary sequence for HIV ds-DNA fragment. As shown in Figure 5a, the fluorescence intensity of the P-DNA decreases upon addition of **2**–**4** with the quenching efficiency (Q_E%) being 4.2% for **2**, 61.8% for **3**, and 22.8% for **4**, and with saturation concentrations of 33.6 μM (**2**), 24.7 μM (**3**) and 30.0 μM (**4**), respectively. Thus, **3** efficiently quenches the photoluminescence of the P-DNA (Figure 5b) due to the formation of P-DNA@**3** system.[3g] For P-DNA is only attached on the surface of compound **3**, the loosely attached P-DNA will fall off during the following sensing assay and largely affect the results. Therefore, we washed the P-DNA@**3** system many times until the fluorescence was not unaltered with the quenching efficiency stabilized at 62%. This is also an optimized condition. With the less amount of **3**, the P-DNA@**3** system will suffer from high background fluorescence of P-DNA. With the excessive **3**, the fluorescence of P-DNA@**3** system could not be recovered.

For comparison, we measured the quenching efficiency of the P-DNA by H_2dcbbBr and $Cu(NO_3)_2$ (Figure 5a and Figure S3). The quenching efficiency (Q_E%) is 17.8% for H_2dcbbBr and 68.8% for $Cu(NO_3)_2$ with the saturation concentrations of 28.3 μM and 43.8 μM. It can be seen that to reach a similar Q_E% to **3**, the $Cu(NO_3)_2$ concentration needs to be nearly doubled. This confirms that the 2D plane structure of **3** is essential to the fluorescence quenching, wherein the interactions between Cu^{2+} and P-DNA may play a major role. This is because the intercalation of Cu^{2+} ions into the P-DNA base pairs and its subsequent electrostatic binding with the phosphate backbone triggers a photoinduced electron transfer (PET) from FAM to Cu^{2+}.[4b-4f] For **2**, the 1D chains of **1** are packed within the cell to generate small channels (Figure 2b), while for **4**, the 1D chains and 2D networks are also packed closely (Figure 4). All these structure characteristics make the P-DNA difficult to form efficient contacts with **2** and **4**.

In the P-DNA@**3** system, addition of the relevant target HIV ds-DNA could lead to the formation of a rigid triplex structure *via* reverse Hoogsteen base pairing in the major groove with the P-DNA.[18] Such triplex DNA formation drives the detachment of the P-DNA from the surface of **3**, leading to the fluorescence regeneration. Thus, the suitability of P-DNA@**3** system as sensing platform for HIV ds-DNA can be evaluated *via* the fluorescence recovery profile upon addition of the complementary duplex HIV ds-DNA. The results indicate that the fluorescence intensity could recover in the presence of target DNA in the P-DNA@**3** system (Figure 5c), but otherwise for P-DNA@$Cu(NO_3)_2$ (Figure S4). This is likely due to the strong interactions between Cu^{2+} and P-DNA in the P-DNA@$Cu(NO_3)_2$ case.[4] For P-DNA@**3** system, we further found that the fluorescence recovery efficiency was time-dependent. The fluorescence intensity increased with incubation time and remained unaltered after 90 min (Figure S5). This time-dependence is indicative of a thermodynamically controlled process. Thus, 90 min incubation time was chosen as one of the operational conditions. Upon addition of target DNA, the fluorescence intensity increases gradually until saturation was observed at the concentration of 120 nM.

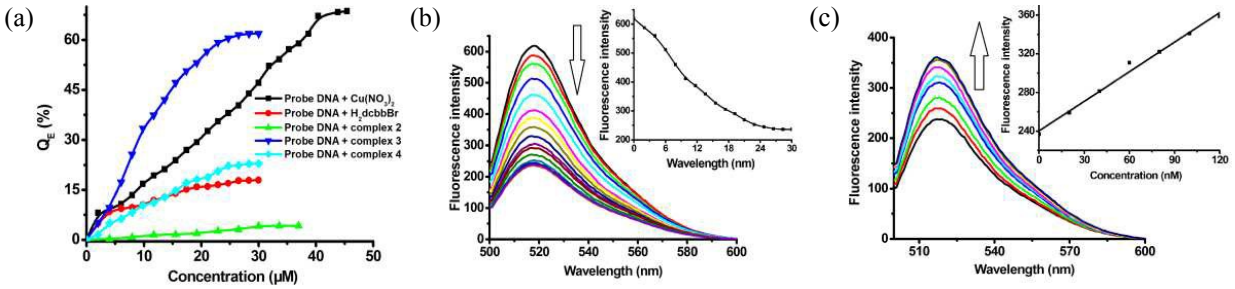

Figure 5. (a) Fluorescence quenching efficiency of the probe DNA (70 nM) by compounds **2**−**4**, H_2dcbbBr and $Cu(NO_3)_2$ of varying concentrations in 100 nM Tris-HCl buffer (pH 7.4) at room temperature. (b) Fluorescence intensity quenching of the probe DNA (70 nM) incubated with compound **3** of varying concentrations at room temperature. Inset: Plot of fluorescence intensity *versus* the concentration of compound **3**. (c) Fluorescent intensity recovery of P-DNA@**3** system after incubation with varying concentrations of target HIV ds-DNA at room temperature. Inset: Plot of fluorescence intensity *versus* target HIV ds-DNA concentration.

Under this condition, the fluorescence intensity shows a good linear relationship with the concentration of target DNA in the range of 1−120 nM (inset of Figure 5(c)). This gave the detection limit of 1.42 nM (S/N = 3), which is comparable to the reported MOF $Cu(H_2dtoa)$ (3.0 nM).[4]

Sequence selectivity assay

The specificity of the sensing platform was investigated by introducing various targets. We chose four types DNA targets, including one base pair mutated ds-DNA T_1, the complementary ss-DNA T_2, one base pair mutated for complementary ss-DNA T_3 and non-specific ss-DNA T_4 to hybridize with the probe DNA in P-DNA@**3** system. Upon addition of the complementary target HIV ds-DNA, T_0, it forms a rigid triplex structure with the probe DNA *via* reverse Hoogsteen base pairing in the major groove.[18] Therefore, the introduction of T_0 results in significant fluorescence enhancement with larger R_E of 0.52, while the use of complementary ss-DNA T_2 provided the R_E of 0.27. At the same concentration, in the presence of one base pair mutated ds-DNA T_1 (one GC base pair was replaced with AT), one base pair mutated for complementary ss-DNA T_3 and non-specific ss-DNA T_4, the R_E are 0.11, 0.19 and 0.09, respectively (Figure 6a). It can be seen from Figure 6b that target ds-DNA T_0 showed much higher fluorescence recovery than the complementary ss-DNA T_2 in a concentration dependent fashion. However, T_1, T_3 and T_4 showed no obvious concentration-dependence. These results indicate that the sensing platform of P-DNA@**3** performs favorably with good specificity for the detection of HIV ds-DNA *in vitro*.

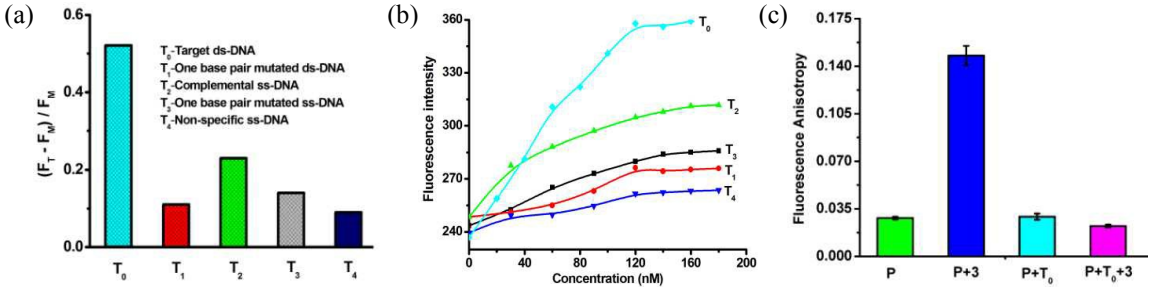

Figure 6. (a) Fluorescence intensity efficiency recovery of the P-DNA@**3** system toward targets DNA T_0 to T_4 at fixed concentration of 120 nM. (b) Fluorescence intensity recovery of the P-DNA@**3** system toward targets DNA T_0 to T_4 with varying concentrations. (c) Fluorescence anisotropy changes of P-DNA (P, 70 nM) incubated for 90 min with compound **3** (24.7 μM), target HIV DNA T_0 (120 nM), a mixture of compound **3** (24.7 μM) and target HIV DNA T_0 (120 nM).

The above results may be rationalized from the unique structure of **3**. Firstly, **3** features a 2D layer structure with large surface area and aromatic rings, positively charged pyridinium and free carboxylates on its surface. Its zeta potential of +8.0 mV indicates that it is positively charged.[3f] Thus, it is reasonable to deduce that **3** can absorb P-DNA through electrostatic, π-stacking and/or hydrogen-bonding interactions to form P-DNA@**3** complex,[19] and thus quench the fluorescence of FAM *via* a PET process (Scheme 1).[20]

Secondly, **3** may have less affinity toward rigid triplex DNA because of the absence of unpaired bases and the rigid conformation of the latter.[17b] The probe ss-DNA is conformationally flexible and should interact with the surface of compound **3** more strongly than rigid triplex DNA. Therefore, the hybridization of T_0 with absorbed probe ss-DNA would lead to the release of labeled dye with the formed triplex DNA into the solution, thus resulting in the recovery of fluorescence (Scheme 1). This assumption is supported by the changes of the fluorescence anisotropy of the P-DNA, P-DNA@target HIV DNA (rigid triplex) before and after the addition of **3**. It is known that fluorescence anisotropy can be a measure for the rotational motion-related factors of fluorophore-labeled DNA,[21] and thus provide a means to judge whether P-DNA and P-DNA@target HIV ds-DNA are attached to the surface of compound **3**. As shown in Figure 6c, the addition of compound **3** into P-DNA leads to an increase in the fluorescence anisotropy by factors of 5.2 for probe DNA whereas a negligible influence on the P-DNA@HIV DNA. This result reveals the strong interaction of compound **3** with P-DNA rather than with rigid triplex DNA.

Journal Name

ARTICLE

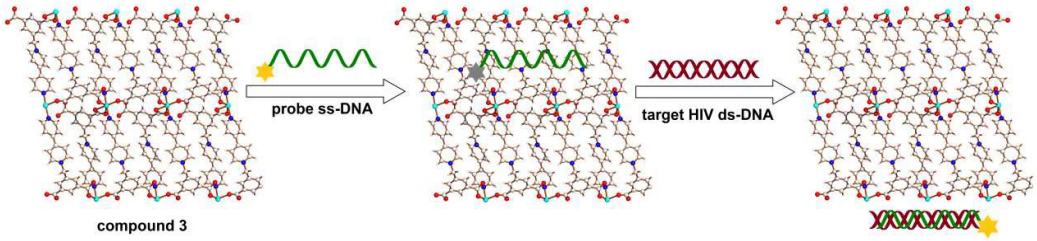

Scheme 1. Mechanism for the detection of target HIV ds-DNA sequences based on a fluorescent biosensor formed from compound **3** and fluorophore-labeled probe DNA.

Conclusions

We described herein a unique polymorphic system containing three compounds **2**, **3** and **4**, wherein **4** is a co-crystal of **2** and **3**. It turned out that the 2D network structure of **3** is more effective in HIV DNA sensing than those of the 1D chain of **1** and the 1D/2D co-crystal of **4**. Such drastic difference can be traced back to their structural characteristic wherein the 2D layer has a higher exposure surface with functional groups to form interactions with probe ss-DNA. This work provides a clue for our future rational design of performer materials. We are currently exploring other 2D systems based on pyridinium carboxylate ligands and their potential in DNA sensing, including HIV DNA and Ebola RNA. These results will be reported in due course.

Acknowledgment

We are grateful for the financial support from the Guangdong Provincial Department of Science and Technology of China (2015A010105016) and Guangdong Provincial Natural Science Foundation of China (2015A030313284), the National Natural Science Foundation of China (Nos. 21102070 and 21401134) and the Program for Pearl River New Stars of Science and Technology in Guangzhou (No. 2011J2200071) and South Medical University.

Notes and references

1. (a) A. Sassolas, B. D. Leca-Bouvier, L. J. Blum, *Chem. Rev.*, 2008, **108**, 109; (b) B. Kannan, D. E. Williams, M. A. Booth, T. S. Jadranka, *Anal. Chem.*, 2011, **83**, 3415; (c) Y. Wang, B. Soontornworajit, *Anal. Bioanal. Chem*., 2011, **399**, 159; (d) M. Larguinho, P. V. Baptista, *J. Proteomics*, 2012, **75**, 2811.
2. (a) Z. Liu, X. L. Li, S. M. Tabakman, K. L. Jiang, S. S. Fan, H. J. Dai, *J. Am. Chem. Soc.*, 2008, **130**, 13540; (b) Y. Chen, H. Liu, T. Ye, J. Kim, C. Mao, *J. Am. Chem. Soc.*, 2007, **129**, 8696; (c) R. Yang, Z. Tang, J. Yan, H. Kang, Y. Kim, Z. Zhu, W. Tan, *Anal. Chem.*, 2008, **80**, 7408; (d) C. H. Lu, H. H. Yang, C. L. Zhu, X. Chen, G. N. Chen, *Angew. Chem. Int. Ed.*, 2009, **48**, 4785; (e) Y. Wen, F. Xing, S. He, S. Song, L. Wang, Y. Long, D. Li, C. Fan, *Chem. Commun.*, 2010, **46**, 2596; (f) Y. Song, K. Qu, C. Zhao, J. Ren, X. Qu, *Adv. Mater.*, 2010, **22**, 2206; (g) L. Zhang, T. Li, B. Li, J. Li, E. Wang, *Chem. Commun.*, 2010, **46**, 1476; (h) H. Li, Y. Zhang, L. Wang, J. Tian, X. Sun, *Chem. Commun.*, 2011, **47**, 961; (i) R. Yang, J. Jin, Y. Chen, N. Shao, H. Kang, Z. Xiao, Z. Tang, Y. Wu, Z. Zhu, W. Tan, *J. Am. Chem. Soc.,* 2008, **130**, 8351; (j) S. Song, Z. Liang, J. Zhang, L. Wang, G. Li, C. Fan, *Angew. Chem. Int. Ed.*, 2009, **48**, 8670; (k) S. Song, Y. Qin, Y. He, Q. Huang, C. Fan, H. Y. Chen, *Chem. Soc. Rev.*, 2010, **39**, 4234; (l) D. A. Giljohann, D. S. Seferos, W. L. Daniel, M. D. Massich, P. C. Patel, C. A. Mirkin, *Angew. Chem. Int. Ed*., 2010, **49**, 3280; (m) Y. Jv, B. Li, R. Cao, *Chem. Commun.,* 2010, **46**, 8017.
3. (a) W. J. Zhang, H. L. Huang, D. H. Liu, Q. Y. Yang, Y. L. Xiao, Q. T. Ma, C. L. Zhong, *Micropor. Mesopor. Mat.,* 2013. **171**, 118; (b) Z. Guo, H. Xu, S. Su, J. Cai, S. Dang, S. Xiang, G. Qian, H. Zhang, M. O'Keeffe, B. Chen, *Chem. Commun.*, 2011, **47**, 5551; (c) G. L. Liu, Y. J. Qin, L. Jing, G. Y. Wei, H. Li. *Chem. Commun.,* 2013, **49**, 1699; (d) F. H. Liu, C. Qin, Y. Ding, H. Wu, K. Z. Shao, Z. M. Su. *Dalton Trans.,* 2015, **44**, 1754; (e) J. M. Fang, F. Leng, X. J. Zhao, X. L. Hua, Y. F. Li, *Analyst*, 2014, **139**, 801; (f) J. F. Guo, C. M. Li, X. L. Hu, C. Z. Huang, Y. F. Li, *RSC Adv.,* 2014, **4**, 9379; (g) H. T. Zhang, J. W. Zhang, G. Huang, Z. Y. Du, H. L. Jiang, *Chem. Commun.,* 2014, **50**, 12069; (h) Y. Wu, J. Han, P. Xue, R. Xu, Y. Kang, *Nanoscale,* 2015, **7**, 1753.
4. (a) X. Zhu, H. Y. Zheng, X. F. Wei, Z. Y. Lin, L. H. Guo, B. Qiu, G. N. Chen, *Chem. Commun.,* 2013, **49**, 1276; (b) B. Gnapareddy, S. J. Ahh, S. R. Dugasani, J. A. Kim, R. Amin, S. B. Mitta, S. Vellampatti, B. Kim, A. Kukarni, T. Kim, K. Yun, T. H. Labean, S. H. Park, *Colloids Surf. B Biointerfaces*, 2015, **135**, 677; (c) S. X. Jiang, H. Yan, Y. Liu, *ACS Nano*, 2014, **8**, 5826; (d) C. Wang, Y. L. Tang, Y. Guo, *ACS Appl. Mater. Interfaces*, 2014, **6**, 21686; (e) E. K. Lim, T. Kim, S. Paik, S. Haam, Y. M. Huh, K. Lee, *Chem. Rev.*, 2015, **115**, 327; (f) J. Zheng, R. Yang, M. Shi, C. Wu, X. Fang, Y. Li, J. Li, W. Tan, *Chem. Soc. Rev.,* 2015, **44**, 3036.
5. (a) L. Chen, H. Zheng, X. Zhu, Z. Lin, L. Guo, B. Qiu, G. Chen, Z. N. Chen, *Analyst,* 2013, **138**, 3490; (b) H. Y. Zheng,

X. M. Ma, L. S. Chen, Z. Y. Lin, L. H. Guo, B. Qiu, G. N. Chen, *Anal. Methods,* 2013, **5**, 5005.

6. (a) J. X. Chen, W. E. Lin, C. Q. Zhou, L. F. Yau, J. R. Wang, B. Wang, W. H. Chen, Z. H. Jiang, *Inorg. Chim. Acta,* 2011, **376**, 389; (b) J. X. Chen, W. E. Lin, M. Z. Chen, C. Q. Zhou, Y. L. Lin, M. Chen, Z. H. Jiang, W. H. Chen, *Bioorg. Med. Chem. Lett.,* 2012, **22**, 7056; (c) C. Q. Zhou, Y. L. Lin, J. X. Chen, W. H. Chen, *Chem. Biodivers.,* 2012, **9**, 1125; (d) C. Q. Zhou, Y. L. Lin, J. X. Chen, L. S. Wang, N. N. Yang, W. Zeng, W. H. Chen, *Bioorg. Med. Chem. Lett.,* 2012, **22**, 5853; (e) M. Z. Chen, M. Chen, C. Q. Zhou, W. E. Lin, J. X. Chen, W. H. Chen, Z. H. Jiang, *Chem. Pharm. Bull.,* 2013, **61**, 714; (f) M. Chen, M. Z. Chen, C. Q. Zhou, W. E. Lin, J. X. Chen, W. H. Chen, Z. H. Jiang, *Inorg. Chim. Acta,* 2013, **405**, 461; (g) J. X. Chen, W. E. Lin, M. Chen, F. C. Que, L. Tao, X. L. Cen, Y. M. Zhou, W. H. Chen, *Inorg. Chim. Acta,* 2014, **409**, 195; (h) Y. M. Wang, C. Q. Zhou, J. X. Chen, Y. L. Lin, W. Zeng, B. C. Kuang, W. L. Fu, W. H. Chen, *Med. Chem. Commun.,* 2013, **4**, 1400; (i) J. X. Chen, M. Chen, N. N. Ding, W. H. Chen, W. H. Zhang, T. S. A. Hor, D. J. Young, *Inorg. Chem*., 2014, **53**, 7446. (j) L. Qin, L. X. Lin, Z. P. Fang, S. P. Yang, G. H. Qiu, J. X. Chen, W. H. Chen, Chem. Commu., 2016, **52**, 132; (k) S. P. Yang, S. R. Chen, S. W. Liu, X. Y. Tang, L. Qin, G. H. Qiu, J. X. Chen, W. H. Chen, *Anal. Chem*., 2015, **87**, 12206.
7. X. Zhu, Y. Liu, J. Yang, Z. Liang, G. Li, *Biosens. Bioelectron.,* 2010, **25**, 2135.
8. G. M. Sheldrick, SADABS, Program for Empirical Absorption Correction of Area Detector Data; University of Göttingen: Göttingen, Germany, 1996.
9. G. M. Sheldrick, SHELXS-97 and SHELXL-97. Programs for Crystal Structure Solution and Refinement; University of Göttingen: Göttingen, Germany, 1997.
10. L. J. Farrugia, *J. Appl. Crystallogr*., 1999, **32**, 837.
11. A. L. Spek, *J. Appl. Crystallogr*., 2003, **36**, 7.
12. (a) M. Ruben, J. Rojo, F. J. Romero-Salguero, L. H. Uppadine, J. M. Lehn, *Angew. Chem. Int. Ed.,* 2004, **43**, 3644; (b) M. E. Carnes, M. S. Collins, D. W. Johnson, *Chem. Soc. Rev.,* 2014, **43**, 1825; (c) M. Lalonde, W. Bury, O. Karagiaridi, Z. Brown, J. T. Hupp, O. K. Farha, *J. Mater. Chem. A,* 2013, **1**, 5453.
13. (a) L. X. Yu, *Pharm. Res.,* 2008, **25**, 781; (b) E. Skořepová, J. Cejka, M. Hušák, V. Eigner, J. Rohlíček, A. Šturc, *Cryst. Growth Des.*, 2013, **13**, 5193; (c) J. F. Remenar, S. L. Morissette, M. L. Peterson, B. Moulton, J. M. Macphee, H. R. Guzmán, O. Almarsson, *J. Am. Chem. Soc.,* 2003, **125**, 8456; (d) F. G. Vogt, G. R. Williams, M. N. Johnson, R. C. B. Copley, *Cryst. Growth Des.,* 2013, **13**, 5353; (e) M. D. Eddleston, B. Patel, G. M. Day, W. Jones, *Cryst. Growth Des.,* 2013, **13**, 4599; (f) B. Moulton, M. J. Zaworotko, *Chem. Rev*., 2001, **101**, 1629; (g) A. V. Trask, W. D. S. Motherwell, W. Jones, *Cryst. Growth Des.,* **2005**, *5*, 1013; (h) H. Moradiya, M. T. Islam, G. R. Woollam, I. J. Slipper, S. Halsey, M. J. Snowden, D. Douroumis, *Cryst. Growth Des.,* 2013, **14**, 189; (i) V. López, J. W. Kampf, A. J. Matzger, *J. Am. Chem. Soc.,* 2012, **134**, 9872; (j) D. K. Bucar, G. M. Day, I. Halasz, G. Z. Zhang, J. R. G. Sander, D. G. Reid, L. R. MacGillivray, M. J. Duer, W. Jones, *Chem. Sci.,* 2013, **4**, 4417.
14. P. Sanphui, S. Tothadi, S. Ganguly, G. R. Desiraju, *Mol. Pharm.,* 2013, **10**, 4687.
15. (a) K. B. Landenberger, O. Bolton, A. J. Matzger, *Angew. Chem. Int. Ed.,* 2013, **52**, 6468; (b) W. Zhu, R. Zheng, X. Fu, H. Fu, Q. Shi, Y. Zhen, H. Dong, W. Hu, *Angew. Chem. Int. Ed*., 2015, **54**, 6785; (c) Q. J. Shen, H. Q. Wei, W. S. Zhou, H. L. Sun, W. J. Jin, *CrystEngComm*., 2012, **14**, 1010; (d) T. Friščić, *Chem. Soc. Rev.,* 2012, **41**, 3493; (e) J. Zhang, J. Tan, Z. Ma, W. Xu, G. Zhao, H. Geng, C. Di, W. Hu, Z. Shuai, K. Singh, D. Zhu, *J. Am. Chem. Soc.,* 2013, **135**, 558; (f) D. Yan, A. Delori, G. O. Lloyd, T. Friščić, G. M. Day, W. Jones, J. Lu, M. Wei, D. G. Evans, X. Duan, *Angew. Chem. Int. Ed.,* 2011, **50**, 12483; (g) T. T. Ong, P. Kavuru, T. Nguyen, R. Cantwell, Ł. Wojtas, M. J. Zaworotko, *J. Am. Chem. Soc.,* 2011, **133**, 9224; (h) S. Aitipamula, R. Banerjee, A. K. Bansal, K. Biradha, M. L. Cheney, A. R. Choudhury, G. R. Desiraju, A. G. Dikundwar, R. Dubey, N. Duggirala, P. P. Ghogale, S. Ghosh, P. K. Goswami, N. R. Goud, R. R. K. R. Jetti, P. Karpinski, P. Kaushik, D. Kumar, V. Kumar, B. Moulton, A. Mukherjee, G. Mukherjee, A. S. Myerson, V. Puri, A. Ramanan, T. Rajamannar, C. M. Reddy, N. Rodriguez-Hornedo, R. D. Rogers, T. N. G. Row, P. Sanphui, N. Shan, G. Shete, A. Singh, C. C. Sun, J. A. Swift, R. Thaimattam, T. S. Thakur, R. K. Thaper, S. P. Thomas, S. Tothadi, V. R. Vangala, N. Variankaval, P. Vishweshwar, D. R. Weyna, M. J. Zaworotko, *Cryst. Growth Des.,* 2012, **12**, 2147.
16. (a) Y. Cui, Y. Yue, G. Qian, B. Chen, *Chem. Rev.,* 2012, **112**, 1126; (b) G. Y. Wang, C. Song, D. M. Kong, W. J. Ruan, Z. Chang, Y. Li, *J. Mater. Chem. A,* 2014, **2**, 2213; (c) W. Morris, W. E. Briley, E. Auyeung, M. D. Cabeas, C. A. Mirkin, *J. Am. Chem. Soc.,* 2014, **136**, 7261.
17. (a) A. Taki, B. John, S. Arakawa, M. Okamoto, *Eur. Polym. J.,* 2013, **49**, 923; (b) ENCODE Project Consortium, *Nature* 2012, **489**, 57; (c) M. Kellis, B. Wold, M. P. Snyder, B. E. Bernstein, A. Kundaje, G. K. Marinov, L. D. Ward, E. Birney, G. E. Crawford, J. Dekker, L. Dunham, L. L. Elnitski, P. J. Farnham, E. A. Feingold, M. Gerstein, M. C. Giddings, D. M. Gilbert, T. R. Gingeras, E. D. Green, R. Guigo, T. Hubbard, J. Kent, J. D. Lieb, R. M. Myers, M. J. Pazin, B. Ren, J. A. Stamatoyannopoulos, Z. Weng, K. P. White, R. C. Hardison, *Proc. Natl. Acad. Sci.*, 2014, **111**, 6131.
18. (a) H. E. Moser, P. B. Dervan, *Science,* 1987, **238**, 645; (b) V. Sklenár, J. Feigon, *Nature,* 1990, **345**, 836; (c) H. Kaur, B. R. Babu, S. Maiti, *Chem. Rev.,* 2007, **107**, 4672; (d) A. Patterson, F. Caprio, A. Vallée-Bélisle, D. Moscone, K. W. Plaxco, G. Palleschi, F. Ricci, *Anal. Chem.,* 2010, **82**, 9109; (e) L. M. Zanoli, R. D'Agata, G. Spoto, *Anal. Bioanal. Chem.,* 2012, **402**, 1759; (f) M. K. Graham, P. S. Miller, *J. Biol. Inorg. Chem.,* 2012, **17**, 1197.
19. (a) C. Lou, A. Dallmann, P. Marafini, R. Gao, T. Brown, *Chem. Sci.,* 2014, **5**, 3836; (b) W. Morris, W. E. Briley, E. Auyeung, M. D. Cabezas, C. A. Mirkin, *J. Am. Chem. Soc.,* 2014, **136**, 7261; (c) X. F. Wei, L. Y. Zheng, F. Luo, Z. Y. Lin, L. H. Guo, G. N. Chen, *J. Mater. Chem. B,* 2013, **1**, 1812; (d) J. X. Chen, H. Q. Zhao, H. H. Li, S. L. Huang, N. N. Ding, W. H. Chen, D. J. Young, W. H. Zhang, T. S. A. Hor, *CrystEngComm*., 2014, **16**, 7722.
20. (a) A. J. M. Huxley, M. Schroeder, H. Q. N. Gunaratne, A. P.

Silva, *Angew. Chem. Int. Ed.,* 2014, **53**, 3696; (b) A. P. de Silva, H. Q. N. Gunaratne, T. Gunnlaugsson, A. J. M. Huxley, C. P. McCoy, J. T. Rademacher, T. E. Rice, *Chem. Rev*., 1997, **97**, 1515.

21. (a) M. E. McCarroll, F. H. Billiot, I. M. Warner, *J. Am. Chem. Soc*., 2001, **123**, 3173; (b) M. Zou, Y. Chen, X. Xu, H. Huang, F. Liu, N. Li, *Biosens. Bioelectron*., 2012, **32**, 148; (c) X. Wang, M. Zou, H. Huang, Y. Ren, L. Li, X. Yang, N. Li, *Biosens. Bioelectron*., 2013, **41**, 569.

Pictogram of Graphical Abstract

A zwitterionic 1D/2D polymer co-crystal and its polymorphic sub-components: a highly selective sensing platform for HIV ds-DNA sequences

Hai-Qing Zhao, Shui-Ping Yang, Ni-Ni Ding, Liang Qin, Gui-Hua Qiu, Jin-Xiang Chen,*[a] Wen-Hua Zhang,* Wen-Hua Chen* and T. S. Andy Hor*